BIOCHEMISTRY

 Volume 46, Number 3 January 23, 2007

Accelerated Publications

Catalytic Mechanism of a MYST Family Histone Acetyltransferase†

Christopher E. Berndsen,‡ Brittany N. Albaugh,‡ Song Tan,§ and John M. Denu*,‡

Department of Biomolecular Chemistry, University of Wisconsin School of Medicine and Public Health, Madison, Wisconsin 53706, and Center for Gene Regulation, Department of Biochemistry and Molecular Biology, Pennsylvania State University, University Park, Pennsylvania 16802

Received December 5, 2006; Revised Manuscript Received December 13, 2006

ABSTRACT: Distinct catalytic mechanisms have been proposed for the Gcn5 and MYST histone acetyltransferase (HAT) families. Gcn5-like HATs utilize an ordered sequential mechanism involving direct nucleophilic attack of the *N*-ϵ-lysine on the enzyme-bound acetyl-CoA. Recently, MYST enzymes were reported to employ a ping-pong route of catalysis via an acetyl−cysteine intermediate. Here, using the prototypical MYST family member Esa1, and its physiological complex (piccolo NuA4), steady-state kinetic analyses revealed a kinetic mechanism that requires the formation of a ternary complex prior to catalysis, where acetyl-CoA binds first and CoA is the last product released. In the absence of histone acceptor, slow rates of enzyme auto-acetylation (7×10^{-4} s^{-1}, or ~2500-fold slower than histone acetylation; $k_{cat} = 1.6$ s^{-1}) and of CoA formation (0.0021 s^{-1}) were inconsistent with a kinetically competent acetyl−enzyme intermediate. Previously, Cys-304 of Esa1 was the proposed nucleophile that forms an acetyl−cysteine intermediate. Here, mutation of this cysteine (C304A) in Esa1 or within the piccolo NuA4 complex yielded an enzyme that was catalytically indistinguishable from the wild type. Similarly, a pH rate (k_{cat}) analysis of the wild type and C304A revealed an ionization ($pK_a = 7.6-7.8$) that must be unprotonated. Mutation of a conserved active-site glutamate (E338Q) reduced k_{cat} ~200-fold at pH 7.5; however, at higher pH, E338Q exhibited nearly wild-type activity. These data are consistent with Glu-338 (general base) activating the *N*-ϵ-lysine by deprotonation. Together, the results suggest that MYST family HATs utilize a direct-attack mechanism within an Esa1·acetyl-CoA·histone ternary complex.

Post-translational modification of histones is linked to a multitude of cellular processes, including transcriptional regulation, DNA damage repair, and DNA replication (*1*−*3*). One prominent histone modification, *N*-ϵ-lysine acetylation, is dynamically controlled by the opposing actions of histone acetyltransferases (HATs)[1] and deacetylases (HDACs) (*2*). The two main families of HATs that comprise the Gcn5-related *N*-acetyltransferase (GNAT) superfamily are the Gcn5 family and the MYST (MOZ, Ybf2/Sas3, Sas2, Tip60)

† This work was supported in part by NIH Grant GM059785 to J.M.D. and NIH Grant GM064089 to S.T.

* To whom correspondence should be addressed: Department of Biomolecular Chemistry, University of Wisconsin School of Medicine and Public Health, 551 Medical Sciences Center, 1300 University Ave., Madison, WI 53706. Phone: (608) 265-1859. Fax: (608) 262-5253. E-mail: jmdenu@wisc.edu.

‡ University of Wisconsin.

§ Pennsylvania State University.

[1] Abbreviations: HAT, histone acetyltransferase; DTT, dithiothreitol; GNAT, Gcn5-related *N*-acetyltransferase; MYST, MOZ, Ybf2/SAS3, SAS2, Tip60; SDS−PAGE, sodium dodecyl sulfate−polyacrylamide gel electrophoresis; picNuA4, piccolo NuA4 histone acetyltransferase complex; MALDI TOF/TOF, matrix-assisted laser desorption ionization time-of-flight/time-of-flight mass spectrometry; AcCoA, acetyl-CoA; HDAC, histone deacetylase.

10.1021/bi602513x CCC: $37.00
Published on Web 12/23/2006

family (*3*−*6*). The Gcn5 family of HATs includes Gcn5 and p/CAF which have well-established sequential mechanisms of acetylation (*7*−*10*). Following the formation of a ternary complex of acetyl-CoA, histone, and enzyme, an active-site base deprotonates lysine, allowing direct attack of the *N*-ϵ-lysine on the carbonyl carbon of acetyl-CoA. A direct acetyl-transfer mechanism contrasts with that recently proposed for the MYST family member from *Saccharomyces cerevisiae*, Esa1 (*11*).

The core structure of Esa1 is significantly similar to that of the Gcn5 HAT family, and accordingly, the first structural report proposed a catalytic mechanism analogous to that established for Gcn5-like HATs (*7*−*10*, *12*−*16*). The most recent crystal structure of Esa1 truncated at residues 160−435 ($Esa1_{160-435}$) revealed the presence of an acetylated cysteine residue (Cys-304) at the putative active site (*11*). This observation and the fact that Cys-304 is invariant among MYST members led to the proposal that Esa1 and all MYST family HATs utilized a catalytic mechanism requiring the formation of a discrete acetyl−cysteine intermediate (*4*, *11*). However, utilization of a poorly active, truncated form of Esa1 and the structural similarity between Esa1 and Gcn5-like HATs raise significant questions about the catalytic mechanism.

Here, we investigate the catalytic mechanism using piccolo NuA4 (picNuA4), a trimeric complex composed of full-length Esa1 as well as two accessory proteins, Epl1 and Yng2, that constitute the minimal core complex capable of efficient histone acetylation (refs *17* and *18* and a manuscript submitted for publication). Previous biochemical analysis of a variety of Esa1 constructs indicated that the catalytic activity is 100−1000-fold lower than that of picNuA4 (*17*). Therefore, we chose to examine this physiologically relevant enzyme complex, which displays catalytic activity similar to that observed for members of the Gcn5 HAT family (*8*−*10*). We demonstrate that Cys-304 is completely dispensable for substrate binding and catalysis and provide evidence that Esa1 employs a direct-attack mechanism from a ternary complex. Moreover, we provide evidence that the conserved active-site Glu-338 deprotonates the *N*-ϵ-lysine of histone, facilitating the nucleophilic attack on the bound acetyl-CoA. This detailed functional analysis suggests that MYST family HATs utilize a direct-attack mechanism (sequential), similar to that established for the Gcn5 HAT family. These results have important implications for the rational design of mechanism-based inhibitors for the entire family of MYST HATs.

EXPERIMENTAL PROCEDURES

Chemicals and Reagents. DTT, Tris base, acetyl-CoA, and other reagents were purchased from Sigma-Aldrich or Fisher; DTNB was purchased from Pierce, and acrylamide/bisacrylamide was purchased from Bio-Rad. All reagents were of the highest quality and used without further purification.

Purification of picNuA4, Esa1, and Mutants. Purification of enzymes was performed as described by Selleck et al. (*18*). Bradford and activity assays were used to determine the enzyme concentration (*19*).

Histone Acetyltransferase Assays. Assays were performed as described by Berndsen and Denu (*20*). All reaction mixtures contained 50 mM Tris (pH 7.5) and were performed at 25 °C using a peptide corresponding to the 20 N-terminal residues of histone H4, SGRGKGGKGLGKGGAKRHRK. The peptide concentration was determined by amino acid analysis (Molecular Structure Facility at the University of California, Davis, CA) and by BCA assay.

Experiments with propionyl-CoA as the substrate were performed using the DTNB assay. Reactions were performed in 50 mM Tris at pH 7.5 and 25 °C with 1 mM EDTA, 0.1 μM picNuA4, 10−100 μM propionyl-CoA, and 36−550 μM $H4_{1-20}$. Reactions were quenched in 10% SDS and 4 mg/mL DTNB in 50 mM Tris (pH 7.5) and 1 mM EDTA. Absorbance was measured in a 384-well plate using a Multiskan Ascent plate reader (Thermo Scientific, Waltham, MA).

pH Profiles. Assays for determining the rate of catalysis over a pH range were performed as described above with 75 μM acetyl-CoA and 1 mM $H4_{1-20}$ in each reaction. The assays were buffered with either 50 mM Tris, 50 mM bis-Tris, and 100 mM sodium acetate or 50 mM Tris, 50 mM ethanolamine, and 100 mM ACES. These buffers have been shown to have a constant ionic strength over a wide pH range (*21*). The picNuA4 complex exhibited similar levels of activity in both buffers.

Mutagenesis. The C304A, C304S, and E338Q mutations were introduced separately into the Esa1 gene in the pST50Trc3-yEsa1 plasmid using the QuikChange mutagenesis procedure. The entire Esa1 coding region was verified by sequencing before the Esa1 translational cassette was subcloned to create pST44 bacterial expression vectors that coexpress His-tagged Epl1(51−380), Yng2(1−218), and Esa1 containing the point mutation (*18*, *23*).

Data Fitting. Data from bisubstrate analysis and inhibition assays were fitted to the equations (eqs 1 and 2, respectively) of Cleland in Kinetasyst (Intellikinetics, State College, PA) as described previously (*8*, *9*). The pH rate data were fitted to eq 3 (*22*), where C is the pH-independent rate, [H] is the concentration of protons, and K_a is the acid dissociation constant. All data were displayed using Kaleidagraph (Synergy Software, Reading, PA).

$$v = (V_m AB)/(K_{ia}K_b + K_{ma}B + K_{mb}A + AB) \quad (1)$$

$$v = (V_m[S])/[K_m(1 + I/K_{is}) + [S]] \quad (2)$$

$$v = \log\left(\frac{C}{1 + \frac{[H]}{K_a}}\right) \quad (3)$$

Mass Spectrometry of Peptides. Esa1 C304A and C304S mutants were confirmed by mass spectrometry. The picNuA4 complex was resolved via SDS−PAGE, and the band corresponding to Esa1 was excised. Gel pieces were reduced, alkylated, and digested with trypsin using standard protocols, and samples were further processed for MALDI by Omix tip (Varian, Inc.). MALDI TOF/TOF was performed at the University of Wisconsin Biotechnology Center on a 4800 MALDI TOF/TOF instrument (Applied Biosystems, Foster City, CA).

RESULTS

Steady-State Kinetic Analysis of picNuA4 Suggests an Ordered Sequential Mechanism. For the mechanistic inves-

tigation reported in this study, we utilized purified, recombinant piccolo trimeric complex picNuA4, containing the full-length catalytic subunit Esa1, and subunits Yng2 and Epl1, which is the minimal core enzyme capable of efficient nucleosomal acetylation (*17*, *18*). Where appropriate, we also report results from full-length Esa1 that is not complexed with Yng2 and Epl1. To distinguish between direct-attack (sequential) and obligate acetyl−cysteine enzyme intermediate (ping-pong) mechanisms, a steady-state kinetic analysis was performed. Initial rates of product formation were determined at varied concentrations of both substrates, acetyl-CoA and a histone H4 peptide ($H4_{1-20}$) corresponding to residues 1−20, and the rate data were plotted in double-reciprocal format (Lineweaver−Burk). Figure 1A shows a representative data set, demonstrating an intersecting line pattern, consistent with a sequential mechanism and the requirement for ternary complex formation prior to catalysis. The k_{cat} value of 1.8 ± 0.6 s^{-1} was determined, with a K_m for acetyl-CoA of 0.9 ± 0.3 μM (K_d = 1.2 ± 0.4 μM) and a K_m for $H4_{1-20}$ of 192 ± 63 μM (K_d = 251 ± 46 μM).

To confirm the observed intersecting line pattern in the bisubstrate analysis, we utilized the approach of employing an alternate acyl-CoA substrate (higher K_m), similar to that performed by Radika and Northrop, who determined a sequential mechanism for kanamycin acetyltransferase (*24*). Here proprionyl-CoA was used, revealing higher K_m (24 ± 11 μM) and K_d (130 ± 6 μM) values, compared to those of acetyl-CoA. The double-reciprocal plot with varied $H4_{1-20}$ and proprionyl-CoA displayed a pronounced intersecting line pattern, demonstrating a strong effect of $H4_{1-20}$ concentration on the k_{cat}/K_m for propionyl-CoA. This dependence is represented in the replot of K_m/k_{cat} for propionyl-CoA versus $1/[H4_{1-20}]$ in Figure 1B. The k_{cat} for propionyl-CoA was 1.6 ± 0.3 s^{-1} with a k_{cat}/K_m of (6.5 ± 0.8) × 10^4 M^{-1} s^{-1}, and for $H4_{1-20}$, the k_{cat}/K_m value was (5.5 ± 0.2) × 10^4 M^{-1} s^{-1}.

A characteristic feature of the Gcn5-like HATs is the ability of the product CoA to act as a competitive inhibitor against the substrate acetyl-CoA (*8*, *9*). Because acetyl-CoA is the first substrate to add and CoA is the last product to leave in the kinetic mechanism, acetyl-CoA and CoA compete for the free enzyme form. We performed inhibition analysis using CoA as a product inhibitor of the picNuA4 reaction. A series of initial velocities were measured at saturating levels of $H4_{1-20}$, where acetyl-CoA concentrations were varied at different fixed levels of CoA. The resulting data shown in double-reciprocal format (Figure 1C) produced an intersecting line pattern that converged on the *y*-axis, indicating competitive inhibition. The inhibition constant (K_i) for CoA was 1.8 ± 0.8 μM. Collectively, our steady-state analyses are consistent with a sequential mechanism involving formation of a ternary complex (picNuA4·acetyl-CoA·$H4_{1-20}$) prior to any chemical step in the reaction mechanism.

Cysteine 304 Does Not Mediate Acetyl Transfer. To directly investigate the role of Cys-304 in picNuA4- and Esa1-catalyzed acetyl transfer, we replaced Cys-304 with either alanine or serine in full-length Esa1 and within the trimeric picNuA4 complex. These amino acid substitutions were confirmed by DNA sequencing of the expression plasmids and by mass spectrometry of the expressed, purified protein (Table 1). Mass spectral analysis of tryptic peptides revealed the correct masses of 2198 Da (2141 Da + alkylation) for the wild type (ESADGYNVACILTLPQYQR),

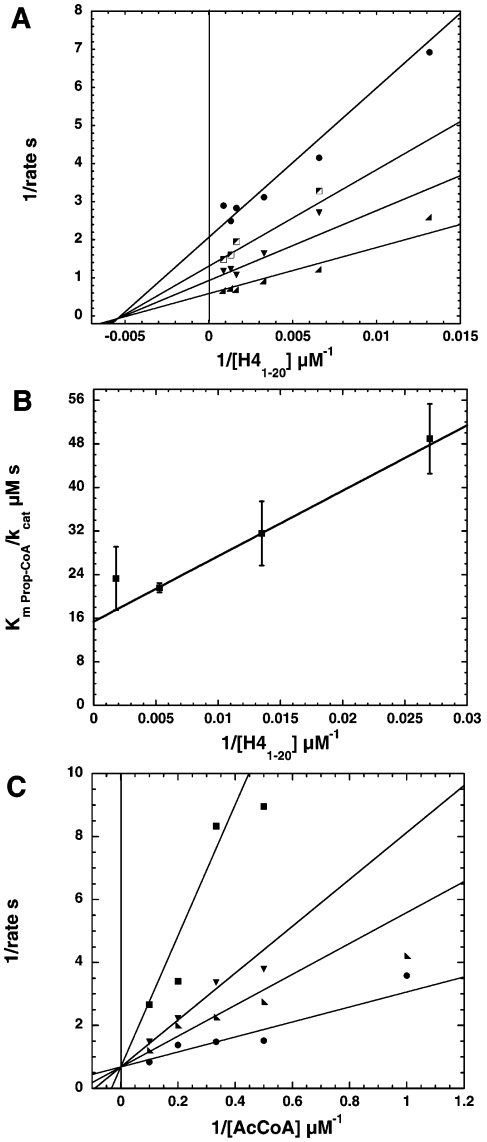

FIGURE 1: picNuA4 requires a ternary complex for histone acetylation. (A) Double-reciprocal plot from a bisubstrate experiment. Acetyltransferase reactions were conducted in 50 mM Tris (pH 7.5), 1 mM DTT, and 0.1 μM picNuA4 with coupled assay conditions as described by Berndsen and Denu (*20*). Acetyl-CoA concentrations are 0.25 (●), 0.5 (◩), 1 (▼), and 10 μM (right triangles) with the $H4_{1-20}$ concentration varied from 50 to 1800 μM. Data were fitted to eq 1 for a sequential mechanism in Kinetasyst and depicted in Kaleidagraph. Experiments were repeated in triplicate with a representative experiment shown. (B) Slope replot from the bisubstrate experiment using propionyl-CoA and $H4_{1-20}$. DTNB assays were conducted in 50 mM Tris (pH 7.5) with 1 mM EDTA with 0.1 μM picNuA4. The propionyl-CoA concentration was varied from 10 to 104 μM with the $H4_{1-20}$ concentration varied from 36 to 550 μM. Curves were fitted to the Michaelis−Menten equation [$v = (V_m[S])/(K_m + [S])$] in Kaleidagraph to determine k_{cat} and k_{cat}/K_m. The $1/(k_{cat}/K_m)$ value with propionyl-CoA was then plotted vs $1/[H4_{1-20}]$. Experiments were repeated in duplicate with average data ± the standard deviation shown. (C) Double-reciprocal plot showing CoA inhibition when the acetyl-CoA concentration is varied at a constant peptide concentration. Reactions were conducted in 50 mM Tris (pH 7.5), 1 mM DTT, 0.03 μM picNuA4, and 500 μM $H4_{1-20}$. The acetyl-CoA concentration was varied from 1 to 10 μM at 0 (●), 2.5 (right triangles), 5 (▼), and 18.2 μM CoA (■). Data were fitted to eq 2 for competitive inhibition and depicted using Kaleidagraph. The K_i for CoA was determined to be 1.8 ± 0.8 μM. Experiments were repeated in duplicate with representative data shown.

Table 1: Kinetic Constants for Piccolo NuA4 and Catalytic Mutants

enzyme	peptide sequence by MS [mass (Da)]	k_{cat} (s^{-1})[a]	K_m(AcCoA) (μM)[a]	$K_{m-peptide}$ (μM)[a]	k_{cat}/K_m(AcCoA) (M^{-1} s^{-1})	$k_{cat}/K_{m-peptide}$ (M^{-1} s^{-1})
WT	ESADGYNVACILTLPQYQR (2141 + alkylation = 2198 Da)	1.6 ± 0.1	2.5 ± 0.3	216 ± 28	$(6.4 \pm 0.9) \times 10^5$	$(7.4 \pm 1.1) \times 10^3$
C304A	ESADGYNVAAILTLPQYQR (2109)	0.76 ± 0.1	1.5 ± 0.2	372 ± 27	$(5.1 \pm 1.0) \times 10^5$	$(2.0 \pm 0.3) \times 10^3$
C304S	ESADGYNVASILTLPQYQR (2125)	0.14 ± 0.02	2.0 ± 0.3	182 ± 34	$(7.0 \pm 1.5) \times 10^4$	$(7.7 \pm 1.8) \times 10^2$
E338Q		$(9.1 \pm 1) \times 10^{-3}$	1.2 ± 0.2	135 ± 10	$(7.6 \pm 1.5) \times 10^3$	$(6.7 \pm 0.9) \times 10$

[a] All values are averages determined from duplicate or triplicate independent experiments shown ± the standard deviation.

2109 Da for C304A (ESADGYNVAAILTLPQYQR), and 2125 Da for C304S (ESADGYNVASILTLPQYQR). The picNuA4 mutants (C304A and C304S) were subjected to steady-state kinetic analysis to determine their effect on all kinetic parameters (Table 1). Strikingly, the C304A mutant of picNuA4 displayed k_{cat} and k_{cat}/K_m values within 3-fold of those determined for wild-type picNuA4 (Table 1). The C304S mutation yielded a 10-fold lower k_{cat} compared to that of wild-type picNuA4, although the K_m values for both substrates were not appreciably affected. Together, these data indicate that Cys-304 does not play an essential catalytic role in the efficient histone acetylation mediated by picNuA4.

To determine if the picNuA4 complex had a compensatory mechanism when Cys-304 was substituted, we determined the effect of the C304A substitution on Esa1 alone. The rates (apparent k_{cat}) of peptide acetylation for Esa1 and the C304A mutant were 0.0019 ± 0.0001 and 0.0015 ± 0.0001 s^{-1}, respectively (data not shown). These results are consistent with the lack of involvement of the Cys-304 sulfhydryl in catalysis by either Esa1 or picNuA4.

Acetylated Piccolo NuA4 Is Not Kinetically Competent. To characterize the auto-acetylation of picNuA4, a variety of biochemical and kinetic experiments were performed. In the presence of [^{14}C]acetyl-CoA, all three proteins, Esa1, Yng2, and Epl1, were labeled with [^{14}C]acetate. Yng2 displayed the highest level of acetyl incorporation, followed by Esa1 and then Epl1 (Figure 1A of the Supporting Information). The acetate incorporated into picNuA4 could not be removed with heat, DTT, β-mercaptoethanol, or CoA, suggesting the formation of a stable linkage that is not consistent with an acetyl−cysteine intermediate (Figure 1B of the Supporting Information and data not shown). Additional attempts to observe picNuA4-catalyzed acetyl exchange between acetyl-CoA and a CoA analogue, 3′-dephospho-CoA, yielded no significant exchange above background levels (data not shown). We next measured the rates of CoA formation in the absence of histone peptide, under either catalytic (nanomolar) or noncatalytic (micromolar) amounts of picNuA4 (Figure 1C,D of the Supporting Information). With catalytic levels of picNuA4, the rate of CoA formation is not significantly higher than that observed for the spontaneous hydrolysis of acetyl-CoA. With micromolar levels of picNuA4, the rate of CoA formed was 0.0021 ± 0.001 s^{-1}. Similarly, the rate of picNuA4 auto-acetylation was $(7 \pm 0.2) \times 10^{-4}$ s^{-1}, or ~2500-fold slower than histone acetylation (Figure 1E of the Supporting Information).

Glutamate 338 Deprotonates the Substrate Lysine. Having provided strong evidence that Esa1 and picNuA4 employ a direct-attack mechanism from a ternary complex, we next sought to identify the general base responsible for activating the attacking lysine nucleophile. In Gcn5, a conserved glutamate residue (Glu-173) was shown to function as a general base, deprotonating the lysine residue for direct attack on the carbonyl of bound acetyl-CoA (*7*, *12*, *25*, *26*). Previously proposed mechanisms for acetyl transfer by Esa1 implicated Glu-338 as being critical for deprotonation of the substrate lysine (*11*, *12*). We constructed an Esa1 E338Q mutant of picNuA4 and investigated its potential role as the general base.

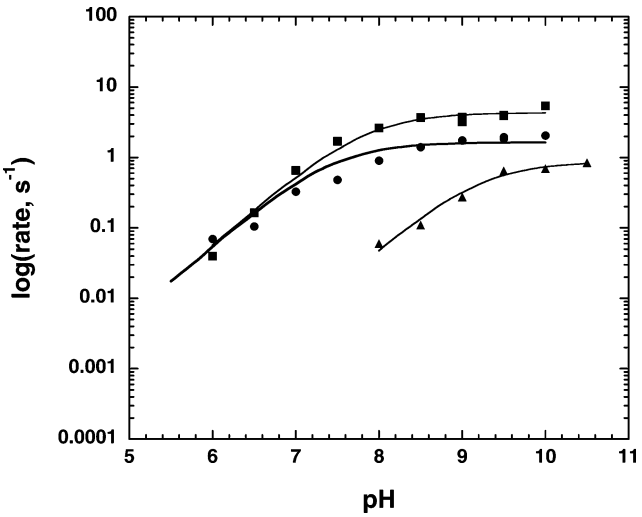

FIGURE 2: pH profile of picNuA4 and mutants. Assays of picNuA4 activity were performed under saturating conditions for both substrates (75 μM acetyl-CoA and 1 mM $H4_{1-20}$). Reactions were performed in either 50 mM Tris, 50 mM bis-Tris, and 100 mM sodium acetate or 50 mM Tris, 50 mM ethanolamine, and 100 mM ACES buffer from pH 5.5 to 10.5. Data for the wild-type enzyme are denoted with squares, those for C304A with circles, and those for E338Q with triangles. Data were fitted to eq 3 and depicted using Kaleidagraph. The pK_a value determined for the wild-type complex was 7.8 ± 0.1, for C304A 7.6 ± 0.2, and for E338Q 9.2 ± 0.1. Experiments were repeated in duplicate or triplicate with representative curves for each enzyme shown.

Steady-state kinetic analysis of the E338Q mutant of picNuA4 indicated that while substrate K_m values for both substrates were similar between the E338Q mutant and wild-type complexes, the k_{cat} of the E338Q mutant was reduced 175-fold at pH 7.5 (Table 1). We next determined the effect of pH on the k_{cat} for wild-type, C304A, and E338Q picNuA4 complexes (Figure 2). The pH profiles for wild-type and C304A complexes were similar, with pK_a values of 7.8 ± 0.1 and 7.6 ± 0.2, respectively, indicating the occurrence of a single ionization that must be unprotonated for catalysis. In contrast, the E338Q mutant displayed a much higher pK_a value of 9.2 ± 0.1 for a single ionization that must be unprotonated for activity. As is evident in Figure 2, the k_{cat} value of the E338Q mutant begins to approach that of the wild-type enzyme at very high pH values. The E338Q mutant data revealed a pH-independent rate of 0.8 ± 0.1 s^{-1}, while those from the C304A and wild-type complexes yielded pH-

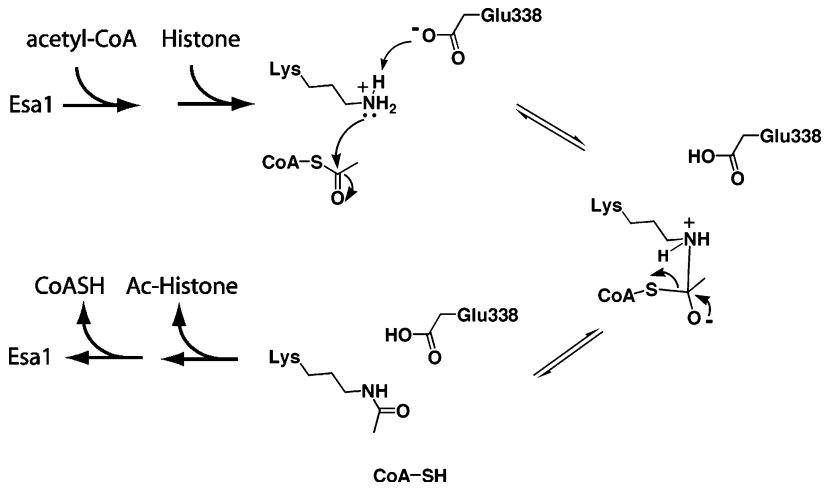

FIGURE 3: Direct-attack mechanism for acetyl transfer by Esa1. After binding acetyl-CoA and peptide substrate to form a ternary complex, glutamate 338 of Esa1 deprotonates the ϵ-amine of lysine in the substrate. Lysine attacks the carbonyl carbon of the acetyl moiety of acetyl-CoA, forming a tetrahedral intermediate, which then collapses to form CoA-SH and acetylated product.

independent values of 1.8 ± 0.2 and 3.9 ± 0.5 s^{-1}, respectively. These results are consistent with a role for Glu-338 as a general base. At physiological pH values, Glu-338 deprotonates the *N*-ϵ-lysine; however, the requirement for Glu-338-catalyzed activation of lysine becomes unnecessary for efficient catalysis at higher pH because the lysine side chain is unprotonated (apparent pK_a of 9.2) (*27*).

DISCUSSION

The catalytic mechanism for the MYST family of HATs has been unresolved (*11*, *12*). Esa1 is used as the prototypical enzyme for understanding the structure and mechanism of the MYST family. Primarily on the basis of the structural similarity to the Gcn5 family of HATs, initial structure determination of the truncated $Esa1_{160-435}$ enzyme suggested a sequential mechanism of acetyl transfer (*12*). However, a subsequent X-ray structure of the same truncated form showed an acetylated cysteine near the active site, serving as primary evidence for the proposal that an acetyl−Cys-304 intermediate is required for catalysis (*11*). Here, we provide detailed functional data demonstrating that the mechanism of Esa1 and picNuA4 does not involve the formation of an acetyl−cysteine 304 intermediate. Instead, the results fully support a ternary complex mechanism involving a direct attack of a deprotonated *N*-ϵ-lysine on the bound acetyl-CoA. Like the Gcn5 HATs, the conserved Glu-338 of Esa1 functions to abstract a proton from lysine to promote the nucleophilic attack on the acetyl carbonyl carbon of acetyl-CoA.

In a previous kinetic bisubstrate analysis, Yan et al. reported a parallel line pattern when $Esa1_{160-435}$ was employed and acetyl-CoA was the acyl donor (*11*). The exact nature of this discrepancy is unclear; however, the low rates of acetylation by the truncated $Esa1_{160-435}$ (~60-fold lower k_{cat}/K_m for peptide) and the narrow range of substrate concentrations used in the previous study may have contributed to this apparent difference and to an assignment of a ping-pong mechanism (*11*). In the study presented here, we observe intersecting line patterns using both acetyl-CoA and proprionyl-CoA as a varied substrate. It is likely that the low K_m and K_d for acetyl-CoA and the technical limitations this presents for the HAT assays may contribute to more subtle intersection line patterns with acetyl-CoA. This issue is alleviated with a poorer (higher K_m) substrate such as propionyl-CoA (Figure 1B), which displayed a pronounced effect on the apparent k_{cat}/K_m for propionyl-CoA at varied peptide concentrations (Figure 1B). Interestingly, the k_{cat} using propionyl-CoA (1.6 s^{-1}) was nearly the same as that for acetyl-CoA (1.8 s^{-1}), suggesting that the rate-limiting step is similar at saturating substrate concentrations. The ability of CoA to competitively inhibit acetyl-CoA provides additional evidence of a sequential mechanism in which acetyl-CoA is the first substrate to bind and CoA is the last product released. In a classical ping-pong mechanism, acetyl-CoA binds first, followed by the transfer of an acetyl to an enzyme nucleophile (*28*). CoA must leave before the peptide lysine binds and reacts with the acetyl−enzyme intermediate, thereby releasing acetylated peptide in the last step. In such a scenario, CoA should exhibit noncompetitive inhibition, which was not observed in our study.

Moreover, if the MYST family HATs utilized an obligate acetyl−enzyme intermediate, there are several predictable outcomes upon reaction of the enzyme with acetyl-CoA. These include the kinetic competence of the acetylated enzyme and the corresponding formation of CoA in the absence of a peptide acceptor (*27*, *29*). While Esa1 is capable of auto-acetylation, this acetylation rate in the absence of peptide was more than 2500-fold slower than the steady-state rate of acetylation (7×10^{-4} s^{-1} vs 1.6 s^{-1}), indicating that the observed acetylation cannot serve as a catalytically competent species (Figure 1E of the Supporting Information). Furthermore, the auto-acetylation of picNuA4 could not be reversed by addition of CoA, suggesting that this inter- or intramolecular acetylation is occurring on lysine residues (Figure 1B of the Supporting Information). Last, the rate of CoA formation (0.0021 s^{-1}) upon reaction of high levels of picNuA4 and acetyl-CoA does not account for a kinetically competent rate (Figure 1C of the Supporting Information). Together, these results argue against an acetyl−enzyme intermediate being involved in the catalytic mechanism.

Contrary to a previously proposed catalytic mechanism, Cys-304 of Esa1 does not function as the nucleophile in a covalent catalysis-type mechanism (*11*). A complete steady-state analysis of the C304A mutant of picNuA4 revealed that

an alanine substitution at this site leads to an almost insignificant change in all kinetic parameters (Table 1). Similarly, the C304A mutant in Esa1 alone exhibited no significant change in the maximum rate of acetylation, compared to full-length wild-type Esa1. The lack of an effect of the C304A substitution suggests that both Esa1 alone and picNuA4 utilize the same catalytic mechanism, one that does not require an acetyl−Cys-304 intermediate. Yan et al. (*11*) reported that the C304A mutation in truncated Esa1$_{160-435}$ resulted in a protein with no detectable activity (*11*). Given our recent finding that Epl1 and Yng2 function to stabilize full-length Esa1 in the picNuA4 complex (manuscript submitted), it appears likely that the C304A mutation may further destabilize Esa1$_{160-435}$, generating an enzyme with background levels of activity (*11*). The slight reduction in the rate of turnover of the C304S complex may be due to this enzyme destabilization. The crystal structure of Esa1$_{160-435}$ with a C304S substitution shows significant structural changes to the loop between α2 and β7, residues 257−271 (PDB entry 1MJ9) (*11*). Mutations in this loop reduce HAT activity, indicating that structural alterations to this loop impact the efficiency of catalysis (*30*). The observation of an acetyl−Cys-304 intermediate in the most recent Esa1$_{160-435}$ crystal structure may have resulted from noncatalyzed reaction of this sulfhydryl with the acetyl-CoA added during crystallization (*11*). Cysteine reactivity is well-established, and nonenzymatic acylation of cysteine residues within peptides by acyl-CoAs has been observed previously (*31*, *32*).

Probing the catalytic role of conserved Glu-338 provides further insight into the mechanism utilized by Esa1. Previously, this residue was proposed to deprotonate Cys-304 and the substrate lysine (*11*). Mutation of this residue to glutamine reduced the rate of turnover by nearly 200-fold at pH 7.5, while the K_m values for both substrates were essentially unchanged (Table 1). However, the E338Q mutant approached near-wild-type k_{cat} values (Figure 2) at higher pH, similar to the behavior observed previously for the general base E173Q mutant of the Gcn5 HAT (*7*). At most physiological pH values, Glu-338 functions as the critical general base by deprotonating the substrate lysine and enhancing catalysis ∼200-fold. In the E338Q mutant, restoration of activity occurs as the *N*-ϵ-lysine (pK_a ∼ 10) becomes unprotonated at higher pH, relinquishing the need for general base catalysis. The pH profiles of both the wild type and the C304A mutant reveal a critical ionization that must be unprotonated for catalysis. Consistent with the general base role of Glu-338, this ionization (pK_a = 7.6−7.8) likely represents the hydrogen-bonded ion pair between Glu-338 and the *N*-ϵ-lysine within the ternary enzyme complex. When this carboxylate is removed in the E338Q mutant, the turnover rate is now dictated by the ionization of the substrate lysine, leading to the higher apparent pK_a of 9.2 (Figure 2).

From the detailed biochemical analysis presented here, we propose the following mechanism for Esa1 and picNuA4-catalyzed transfer of acetyl to histones. After ternary complex formation, Glu-338 abstracts a proton from the substrate lysine, allowing for direct attack on the acetyl moiety of acetyl-CoA (Figure 3). A putative tetrahedral intermediate is formed, which collapses to release CoA and acetylated substrate (Figure 3). These findings reconcile the previously held conclusion that MYST HATs might employ a different catalytic mechanism than other members of the GNAT superfamily (*11*). Instead, our study supports the notion that, despite the disparities in primary structure and substrate specificity between the diverse members of transferase families, GNAT superfamily enzymes use an evolutionarily conserved mechanism of *N*-acyl transfer (*4*).

ACKNOWLEDGMENT

We thank Dr. Alvan Hengge and members of the Denu lab for helpful comments and assistance, especially Dr. Suzi Lee and Brian Smith. Additionally, we thank Jim Brown for assistance with analysis of MALDI spectra.

SUPPORTING INFORMATION AVAILABLE

Data on the characterization of picNuA4 auto-acetylation. This material is available free of charge via the Internet at http://pubs.acs.org.

REFERENCES

1. Doyon, Y., and Cote, J. (2004) The highly conserved and multifunctional NuA4 HAT complex, *Curr. Opin. Genet. Dev. 14*, 147−154.
2. Roth, S. Y., Denu, J. M., and Allis, C. D. (2001) Histone acetyltransferases, *Annu. Rev. Biochem. 70*, 81−120.
3. Sterner, D. E., and Berger, S. L. (2000) Acetylation of histones and transcription-related factors, *Microbiol. Mol. Biol. Rev. 64*, 435−459.
4. Vetting, M. W., LP, S. d. C., Yu, M., Hegde, S. S., Magnet, S., Roderick, S. L., and Blanchard, J. S. (2005) Structure and functions of the GNAT superfamily of acetyltransferases, *Arch. Biochem. Biophys. 433*, 212−226.
5. Marmorstein, R. (2001) Structure of histone acetyltransferases, *J. Mol. Biol. 311*, 433−444.
6. Marmorstein, R. (2001) Structure and function of histone acetyltransferases, *Cell. Mol. Life Sci. 58*, 693−703.
7. Tanner, K. G., Trievel, R. C., Kuo, M. H., Howard, R. M., Berger, S. L., Allis, C. D., Marmorstein, R., and Denu, J. M. (1999) Catalytic mechanism and function of invariant glutamic acid 173 from the histone acetyltransferase GCN5 transcriptional coactivator, *J. Biol. Chem. 274*, 18157−18160.
8. Tanner, K. G., Langer, M. R., Kim, Y., and Denu, J. M. (2000) Kinetic mechanism of the histone acetyltransferase GCN5 from yeast, *J. Biol. Chem. 275*, 22048−22055.
9. Tanner, K. G., Langer, M. R., and Denu, J. M. (2000) Kinetic mechanism of human histone acetyltransferase P/CAF, *Biochemistry 39*, 15652.
10. Lau, O. D., Courtney, A. D., Vassilev, A., Marzilli, L. A., Cotter, R. J., Nakatani, Y., and Cole, P. A. (2000) p300/CBP-associated factor histone acetyltransferase processing of a peptide substrate. Kinetic analysis of the catalytic mechanism, *J. Biol. Chem. 275*, 21953−21959.
11. Yan, Y., Harper, S., Speicher, D. W., and Marmorstein, R. (2002) The catalytic mechanism of the ESA1 histone acetyltransferase involves a self-acetylated intermediate, *Nat. Struct. Biol. 9*, 862−869.
12. Yan, Y., Barlev, N. A., Haley, R. H., Berger, S. L., and Marmorstein, R. (2000) Crystal structure of yeast Esa1 suggests a unified mechanism for catalysis and substrate binding by histone acetyltransferases, *Mol. Cell 6*, 1195−1205.
13. Smith, E. R., Eisen, A., Gu, W., Sattah, M., Pannuti, A., Zhou, J., Cook, R. G., Lucchesi, J. C., and Allis, C. D. (1998) ESA1 is a histone acetyltransferase that is essential for growth in yeast, *Proc. Natl. Acad. Sci. U.S.A. 95*, 3561−3565.
14. Clarke, A. S., Lowell, J. E., Jacobson, S. J., and Pillus, L. (1999) Esa1p is an essential histone acetyltransferase required for cell cycle progression, *Mol. Cell. Biol. 19*, 2515−2526.
15. Bird, A. W., Yu, D. Y., Pray-Grant, M. G., Qiu, Q., Harmon, K. E., Megee, P. C., Grant, P. A., Smith, M. M., and Christman, M.

F. (2002) Acetylation of histone H4 by Esa1 is required for DNA double-strand break repair, *Nature 419*, 411−415.
16. Doyon, Y., Selleck, W., Lane, W. S., Tan, S., and Cote, J. (2004) Structural and functional conservation of the NuA4 histone acetyltransferase complex from yeast to humans, *Mol. Cell. Biol. 24*, 1884−1896.
17. Boudreault, A. A., Cronier, D., Selleck, W., Lacoste, N., Utley, R. T., Allard, S., Savard, J., Lane, W. S., Tan, S., and Cote, J. (2003) Yeast enhancer of polycomb defines global Esa1-dependent acetylation of chromatin, *Genes Dev. 17*, 1415−1428.
18. Selleck, W., Fortin, I., Sermwittayawong, D., Cote, J., and Tan, S. (2005) The *Saccharomyces cerevisiae* Piccolo NuA4 histone acetyltransferase complex requires the Enhancer of Polycomb A domain and chromodomain to acetylate nucleosomes, *Mol. Cell. Biol. 25*, 5535−5542.
19. Bradford, M. M. (1976) A rapid and sensitive method for the quantitation of microgram quantities of protein utilizing the principle of protein-dye binding, *Anal. Biochem. 72*, 248−254.
20. Berndsen, C. E., and Denu, J. M. (2005) Assays for mechanistic investigations of protein/histone acetyltransferases, *Methods 36*, 321−331.
21. Ellis, K. J., and Morrison, J. F. (1982) Buffers of constant ionic strength for studying pH-dependent processes, *Methods Enzymol. 87*, 405−426.
22. Cleland, W. W. (1982) The use of pH studies to determine chemical mechanisms of enzyme-catalyzed reactions, *Methods Enzymol. 87*, 390−405.
23. Tan, S., Kern, R. C., and Selleck, W. (2005) The pST44 polycistronic expression system for producing protein complexes in *Escherichia coli*, *Protein Expression Purif. 40*, 385−395.
24. Radika, K., and Northrop, D. B. (1984) The kinetic mechanism of kanamycin acetyltransferase derived from the use of alternative antibiotics and coenzymes, *J. Biol. Chem. 259*, 12543−12546.
25. Rojas, J. R., Trievel, R. C., Zhou, J., Mo, Y., Li, X., Berger, S. L., Allis, C. D., and Marmorstein, R. (1999) Structure of *Tetrahymena* GCN5 bound to coenzyme A and a histone H3 peptide, *Nature 401*, 93−98.
26. Clements, A., Rojas, J. R., Trievel, R. C., Wang, L., Berger, S. L., and Marmorstein, R. (1999) Crystal structure of the histone acetyltransferase domain of the human PCAF transcriptional regulator bound to coenzyme A, *EMBO J. 18*, 3521−3532.
27. Fersht, A. (1999) *Structure and mechanism in protein science: A guide to enzyme catalysis and protein folding*, pp 170, 216−242, W. H. Freeman, New York.
28. Segel, I. H. (1975) *Enzyme kinetics: Behavior and analysis of rapid equilibrium and steady-state enzyme systems*, pp 653−656, Wiley, New York.
29. Purich, D. L. (2002) Covalent enzyme-substrate compounds: Detection and catalytic competence, *Methods Enzymol. 354*, 1−27.
30. Adachi, N., Kimura, A., and Horikoshi, M. (2002) A conserved motif common to the histone acetyltransferase Esa1 and the histone deacetylase Rpd3, *J. Biol. Chem. 277*, 35688−35695.
31. Quesnel, S., and Silvius, J. R. (1994) Cysteine-containing peptide sequences exhibit facile uncatalyzed transacylation and acyl-CoA-dependent acylation at the lipid bilayer interface, *Biochemistry 33*, 13340−13348.
32. Sang, S. L., and Silvius, J. R. (2005) Novel thioester reagents afford efficient and specific S-acylation of unprotected peptides under mild conditions in aqueous solution, *J. Pept. Res. 66*, 169−180.

BI602513X